

# Shear Alfvén Eigenmodes in Compact Stellarators

D.A. Spong<sup>1</sup>, R. Sanchez<sup>2</sup>, A. Weller<sup>3</sup>, S.P. Hirshman<sup>1</sup>

<sup>1</sup>Oak Ridge National Laboratory, P.O. Box 2009, Oak Ridge, TN 37831-8073

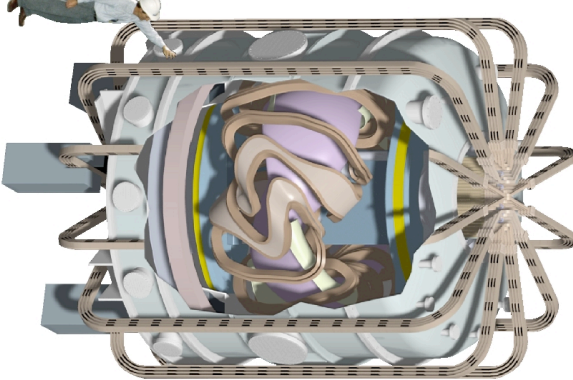
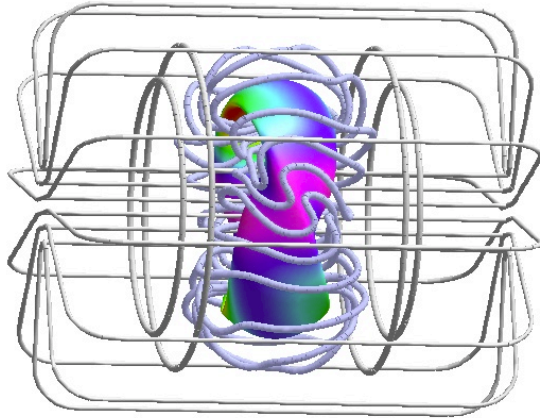
<sup>2</sup>Universidad Carlos III de Madrid, Madrid, Spain

<sup>3</sup>Max-Planck-Institut für Plasmaphysik, IPP-Euratom Association, Garching, Germany

## 13th INTERNATIONAL STELLARATOR WORKSHOP

Australian National University

Canberra, Australia



OAK RIDGE NATIONAL LABORATORY  
U.S. DEPARTMENT OF ENERGY



Max-Planck-Institut  
für Plasmaphysik



# Introduction

- Motivations for analyzing Alfvén instabilities in stellarators
  - Readily seen experimentally (W7-AS, CHS, LHD)
    - A. Weller, D. A. Spong, et al., Phys. Rev. Lett. **72**, 1220 (1994); K. Toi, et al., Nucl. Fusion **40**, 149 (2000); A. Weller, et al., Phys. of Plasmas **8** 931(2001)
  - Can lead to enhanced loss of fast ions
  - Potentially useful as a diagnostic (MHD spectroscopy)
  - Possible catalyst for direct channeling of fast ion energy to thermal ions
- Low aspect ratio configurations provide a new environment for Alfvén studies
  - Stronger equilibrium mode couplings
  - Lower number of field periods lead to
    - More closely coupled toroidal modes ( $n_0, n_0 \pm N_{fp}$ , etc.)
      - This leads to MAE (Mirror Alfvén) and HAE (Helical Alfvén) couplings at lower frequencies

# Ideal MHD Shear Alfvén Equations

$$p_1 + \vec{\square} \cdot \vec{\square} P + \square_s P \vec{\square} \cdot \vec{\square} = 0$$

$$\square^2 \vec{\square} = \vec{\square} p_1 + \vec{b} \square (\vec{\square} \square \vec{B}) + \vec{B} \square (\vec{\square} \square \vec{b})$$

$$+ \vec{\square} \cdot \vec{\mathbf{P}}_{hot}$$

not currently  
included

with  $\vec{\square} = \text{perturbed plasma displacement}$

$p_1 = \text{perturbed pressure}$

$\vec{b} = \vec{\square} \square (\vec{\square} \square \vec{B}) = \text{perturbed } \vec{B} \text{ field}$

[e.g., see I. Bernstein, et al., Proc. Royal Soc. A244, 17(1958) with  $\square_0 = 0$ ]

$$\text{Now, use the variables : } \vec{\square} \cdot \vec{\square}, \quad \square_s = \vec{\square} \cdot \frac{\vec{B} \square \square \vec{\square}}{\left| \vec{\square} \square \right|^2}, \quad \square_l = \vec{\square} \cdot \vec{\square} \square, \quad P_1 = p_1 + \vec{b} \cdot \vec{B}$$

Also, for now take  $\square_s = 0$  and  $\vec{\square} \cdot \vec{\square} = 0$  (incompressible)

This leads to a set of 3 coupled equations. A singularity condition gives the Alfvén continuum [A. Salat, J. A. Tataronis, Phys. Plasmas 8, 1200 (2001); C.Z. Cheng, M. S. Chance, Phys. Fluids 29, 3695 (1986); and other references]

$$\text{where } E_{11} = \frac{\bar{D}^2 |\bar{D} \bar{\bar{D}}|^2}{B^2} + \bar{B} \cdot \bar{\bar{D}} \frac{|\bar{D} \bar{\bar{D}}|^2 \bar{B} \cdot \bar{\bar{D}}}{B^2}$$

$$C_{11} = \bar{D}_{\bar{D}}$$

$$C_{12} = \bar{D}^2 \bar{D} + P \bar{D} \bar{D} + |\bar{D} \bar{D}|^2 \bar{B} \cdot \bar{\bar{D}} \frac{|\bar{D} \bar{\bar{D}}|^2}{B^2} \bar{B} \cdot \bar{\bar{D}}$$

$$+ \frac{|\bar{B} \cdot \bar{J} \bar{D} \bar{D} \bar{S} \bar{D}|^2 |\bar{S} \bar{D} \bar{D}|^2 / B^2}{|\bar{D} \bar{D}|^2}$$

$$C_{22} = |\bar{D} \bar{D}|^2 \bar{D} \bar{D} / |\bar{D} \bar{D}|^2$$

$$D_{11} = |\bar{D} \bar{D}|^2 \bar{D} \bar{D} \bar{B} \cdot \bar{J} \frac{|\bar{D} \bar{D}|^2}{B^2} \bar{B} \cdot \bar{D}$$

$$D_{21} = |\bar{D} \bar{D}|^2 \bar{D} \bar{D} \frac{\bar{B} \bar{D} \bar{D} \bar{D}}{B^2} \cdot \bar{D}$$

$$F_{11} = \bar{D} \bar{D}_s + \frac{\bar{B} \bar{D} \bar{D} \bar{D}}{B^2} \cdot \bar{D}$$

$$F_{21} = \bar{D} \bar{D} / B^2$$

$$F_{12} = \bar{B} \cdot \bar{\bar{D}} \frac{|\bar{D} \bar{D}|^2 S}{B^2} \bar{D} \frac{\bar{J} \cdot \bar{B}}{B^2} \bar{B} \cdot \bar{\bar{D}} \bar{D} P \bar{D}_s$$

$$\begin{aligned} \vec{D} \cdot \vec{D} P &= C_{11} P + C_{12} \bar{D} + D_1 \bar{D}_s \\ \vec{D} \cdot \vec{D} \bar{D} &= C_{22} \bar{D} + D_2 \bar{D}_s \\ E_1 \bar{D}_s &= F_{11} P + F_{12} \bar{D} \end{aligned}$$

Singular for Alfvén continuum condition :  $E_1 \bar{D}_s = 0$

$$\bar{D}_D = 2 \bar{D} \cdot \bar{\bar{D}} \bar{D}, \quad \bar{D}_s = 2 \bar{D} \cdot \bar{B} \bar{D} \bar{D} \bar{D} / |\bar{D} \bar{D}|^2$$

$$S = \text{Local magnetic shear} = \frac{\bar{B} \bar{D} \bar{D} \bar{D}}{|\bar{D} \bar{D}|^2} \cdot \bar{D} \bar{D} \frac{\bar{B} \bar{D} \bar{D} \bar{D}}{|\bar{D} \bar{D}|^2}$$

# Stellarator Alfvén Continuum Equation

The continuum equation in general geometry (low  $\square$ ) can be written:

$$\square_0 \square^2 \frac{|\square \square|^2}{B^2} \square_s + \vec{B} \cdot \vec{\square} \frac{|\square \square|^2}{B^2} (\vec{B} \cdot \vec{\square}) \square_s = 0 \quad (1)$$

This can be written in Boozer coordinates using the following:

$$\vec{B} \cdot \vec{\square} = \frac{1}{\sqrt{g}} \frac{\partial}{\partial \square} + \frac{\partial}{\partial \square} \quad \text{and} \quad |\vec{\square} \square|^2 = g \frac{d \square}{d \square} \square^2$$

For devices with stellarator symmetry, the surface displacement can be expanded as follows:

$$\square_s = \prod_{j=1}^L \square_s^j e_j \quad \text{where} \quad e_j = \cos(n_j \square \square m_j \square)$$

Multiplying equation (1) by the Jacobian and integrating over a flux surface then leads to:

$$\square_0 \square^2 \square \left\langle e_i \sqrt{g} \frac{g \square \square}{B^2} \prod_{j=1}^L \square_j e_j \right\rangle + \left\langle e_i \frac{\partial}{\partial \square} + \frac{\partial}{\partial \square} \frac{g \square \square}{B^2} \frac{\partial}{\partial \square} + \frac{\partial}{\partial \square} \prod_{j=1}^L \square_j e_j \right\rangle = 0$$

# Stellarator Alfvén Continuum Equation (contd.)

Integrating by parts then leads to the following symmetric matrix eigenvalue problem:

$$\square^2 \mathbf{A} \mathbf{x} = \mathbf{B} \mathbf{x}$$

where  $\mathbf{A} = [a_{ij}] = \square_0 \square \left\langle e_i \sqrt{g} \frac{g^{\square\!\square}}{B^2} e_j \right\rangle$

$$\mathbf{B} = [b_{ij}] = \left\langle \frac{g^{\square\!\square}}{B^2 \sqrt{g}} \left[ \frac{\partial e_i}{\partial \square} + \frac{\partial e_i}{\partial \square} \left[ \frac{\partial e_j}{\partial \square} + \frac{\partial e_j}{\partial \square} \right] \right] \right\rangle$$

$$\mathbf{x} = [\square_s \ \square^2_s \cdots \square_s]^T$$

# STELLGAP code

The equilibrium coefficients in the continuum equation can be expanded in cos series:

$$\frac{g}{B^2} \sqrt{g} = \prod_{k=1}^K E_k \cos(n_k \theta \omega m_k \phi), \quad \frac{g}{B^2} \sqrt{g} = \prod_{k=1}^K F_k \cos(n_k \theta \omega m_k \phi)$$

Using these expansions, the matrix elements then can be expressed in terms of the following convolution integrals:

$$I_{ccc}^{i,j,k} = \int_0^{2\pi} \int_0^{2\pi} \int_0^{2\pi} d\theta \int_0^{2\pi} d\theta \int_0^{2\pi} d\phi \cos(n_i \theta \omega m_i \phi) \cos(n_j \theta \omega m_j \phi) \cos(n_k \theta \omega m_k \phi)$$

$$I_{ssc}^{i,j,k} = \int_0^{2\pi} \int_0^{2\pi} \int_0^{2\pi} d\theta \int_0^{2\pi} d\theta \int_0^{2\pi} d\phi \sin(n_i \theta \omega m_i \phi) \sin(n_j \theta \omega m_j \phi) \cos(n_k \theta \omega m_k \phi)$$

# STELLGAP code

Rapid algorithms have been developed that perform the convolution integrals analytically for arbitrary  $m_i, n_i, m_j, n_j, m_k, n_k$ . These have been checked against slower numerical convolution integrators. The final form of the matrix elements is then given as:

$$a_{ij} = \square_0 \square_{ion} \prod_{k=1}^K I_{ccc}^{i,j,k} E_k$$

$$b_{ij} = \prod_{k=1}^K I_{ssc}^{i,j,k} F_k \left[ i^2 m_i m_j + n_i n_j + i(m_i n_j + m_j n_i) \right]$$

The matrix eigenvalue problem is then solved using the IBM ESSL library routine DGEGV which provides all of the eigenvalues for each flux surface. For stellarators, 100-200 equilibrium modes and a similar number of modes for  $\square_s$  are typically used over ~2000 flux surfaces (i.e., 10 - 15 toroidal modes and 10-15 poloidal modes). MPI parallelization is used over the flux surfaces.

# Profiles, mode selection for Alfvén Continuum Plots

- **Profiles used:**

- For W7-AS discharges (42873 and 43348), experimental profiles were used
- Flat ion density  $n_{\text{ion}}(0) = 1 \times 10^{20} \text{ m}^{-3}$
- ion density profile (*iota*)<sup>2</sup> aligns the gaps radially
  - minimizes continuum damping
  - implies a hollow profile for stellarator iota profiles

- **Typical mode selections used:**

Equilibrium

$m = 0 - 19$

$n = -20N_{fp}$  to  $20N_{fp}$

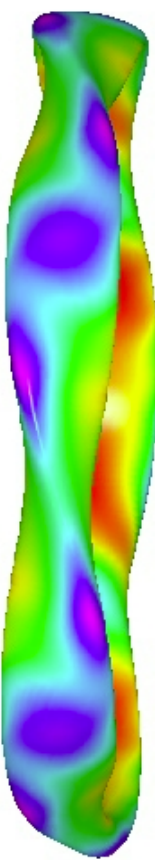
Eigenfunction

$m = 0 - 19$

$n = -4N_{fp} + n_0$  to  $+4N_{fp} + n_0$   
with  $n_0$  = toroidal mode family

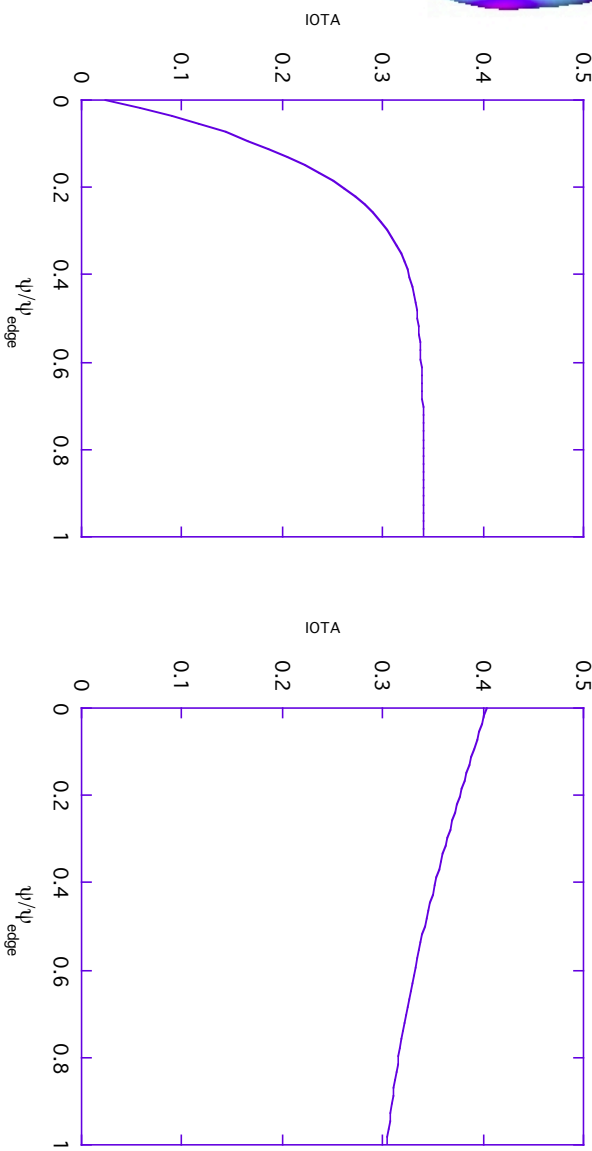
- Nominal design B fields and transform profiles are taken.

# High aspect ratio drift-optimized W7-AS configuration



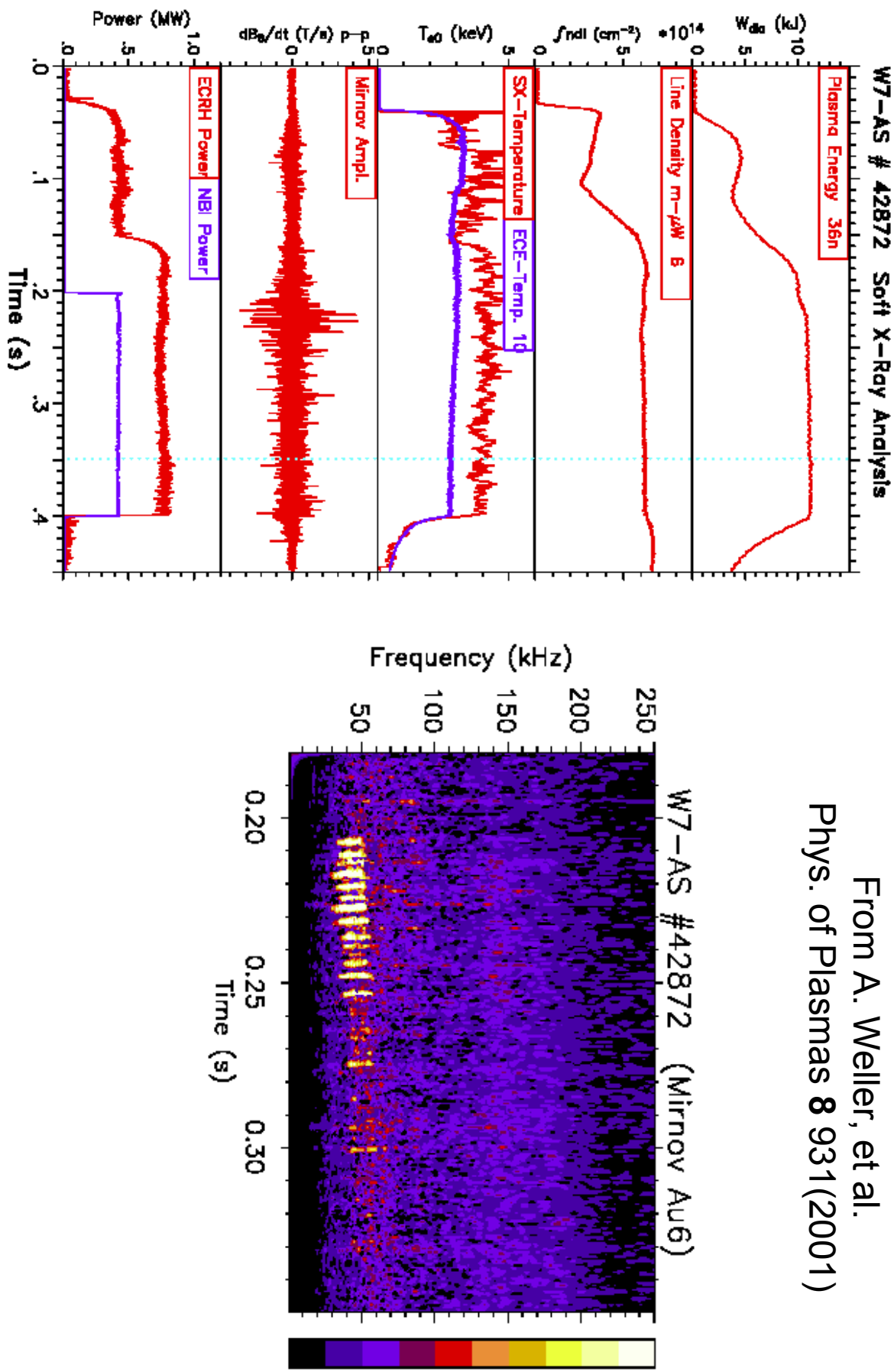
Iota profiles

s42873



# W7-AS Experimental Results for #42872:

From A. Weller, et al.  
Phys. of Plasmas **8** 931(2001)



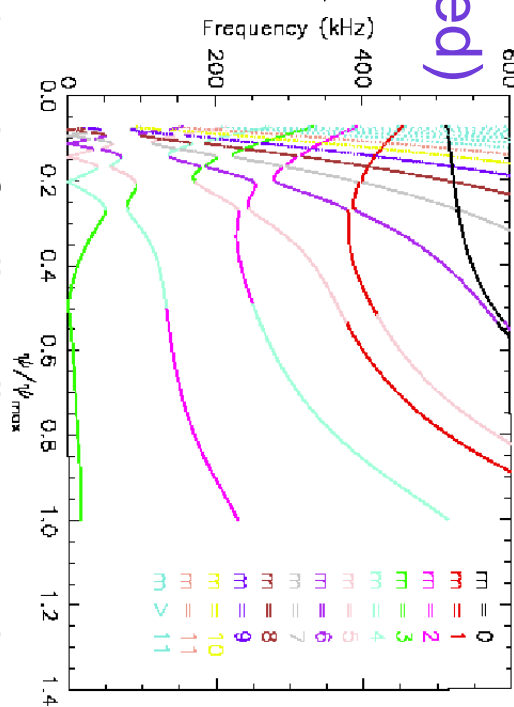
# W7-AS: discharge 42873

(5 field periods  $R/\langle a \rangle = 12$ , drift optimized)

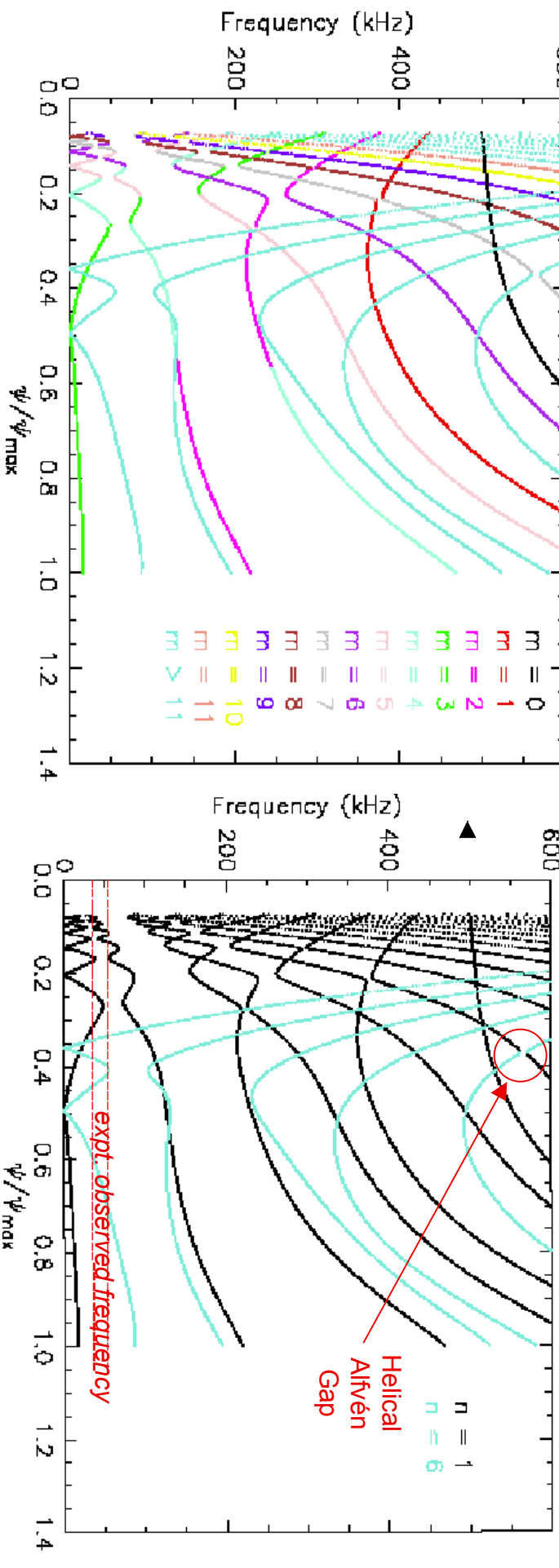
Continuum structure with 3D equilibrium coefficients, but only one ( $n = 1$ ) toroidal mode

Continua with multiple toroidal modes

$n = 1$  mode family stellarator continua  
dominant poloidal mode is color coded

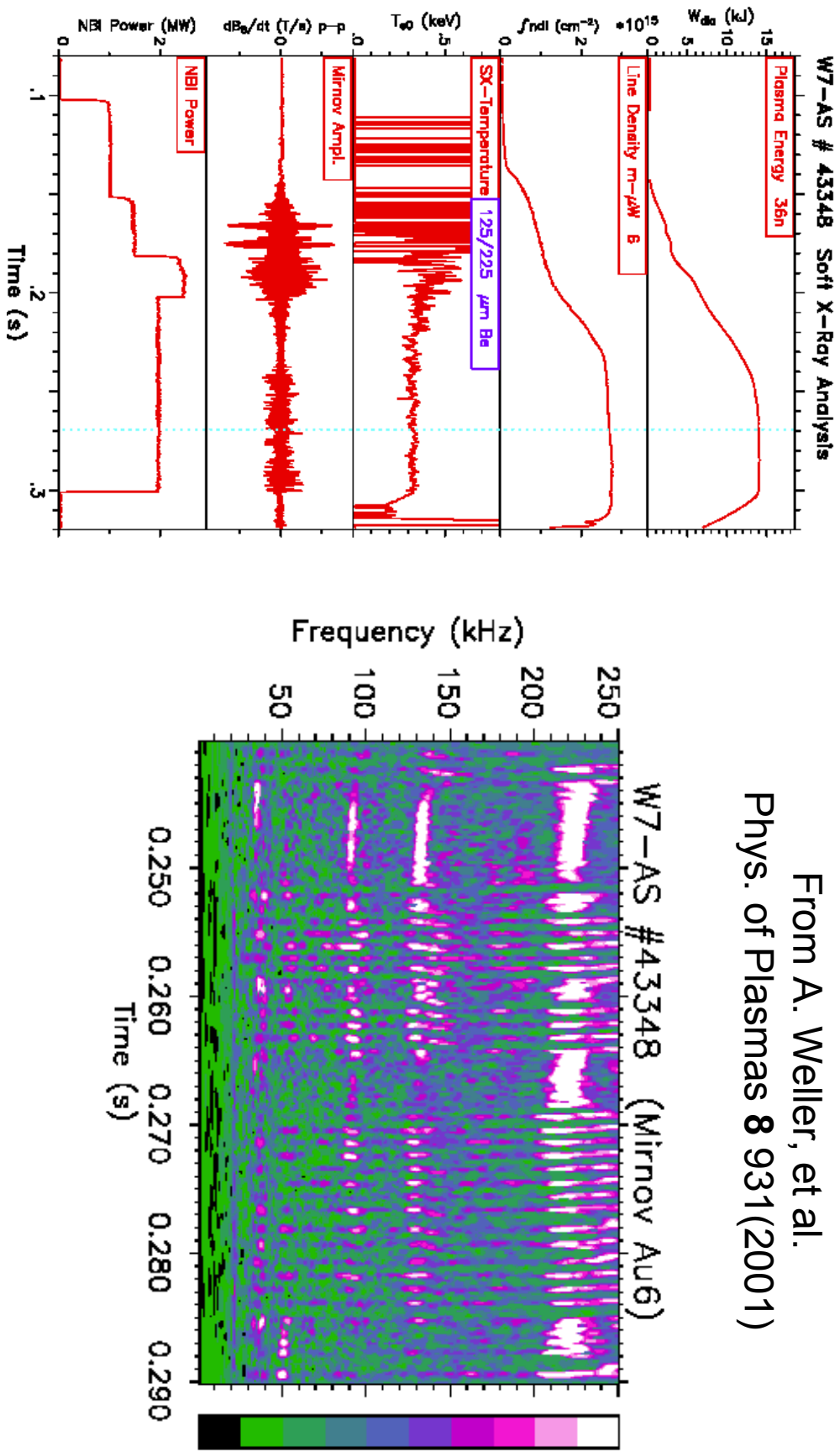


$n = 1$  mode family stellarator continua  
dominant toroidal mode is color coded



# W7-AS Experimental Results for #43348:

From A. Weller, et al.  
Phys. of Plasmas 8 931(2001)



# W7-AS: discharge 43348 (5 field periods

$R/\langle a \rangle = 12$ , drift optimized)

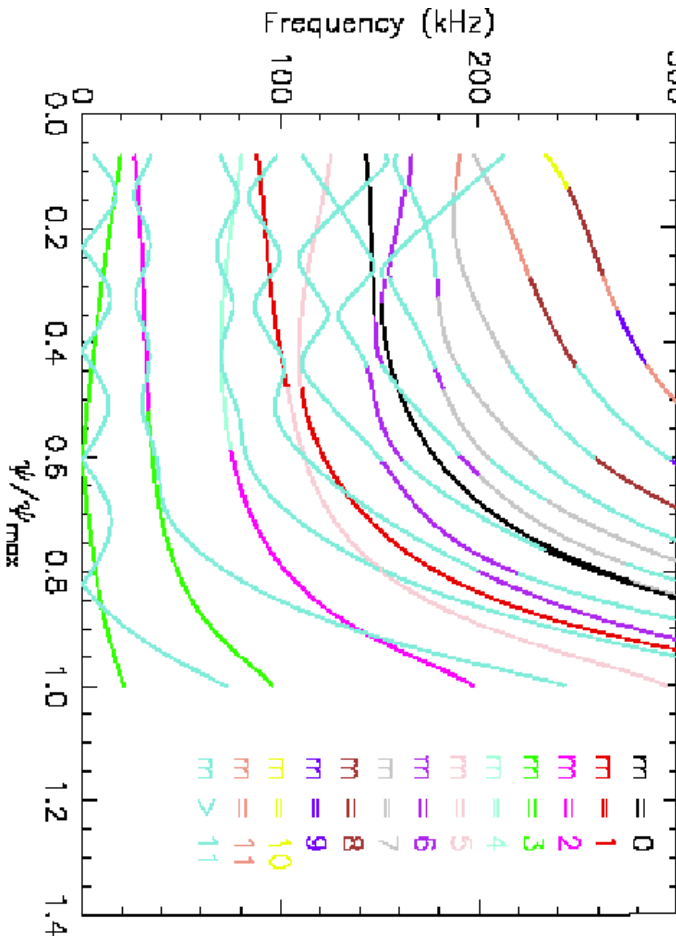
Continuum structure with 3D equilibrium coefficients, but only one ( $n = 1$ ) toroidal mode

Continua with multiple toroidal modes



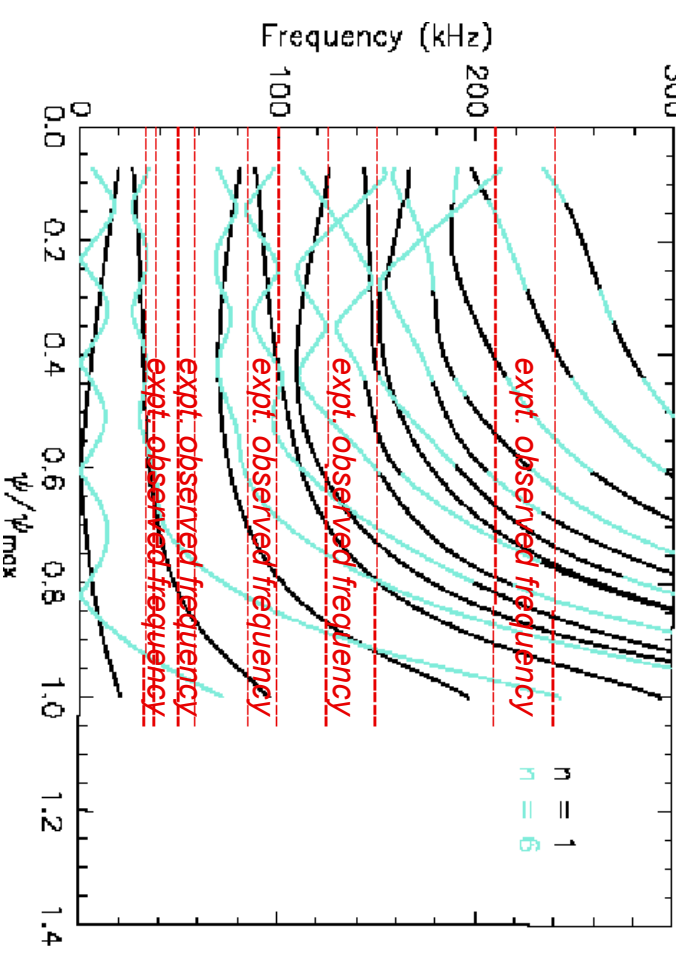
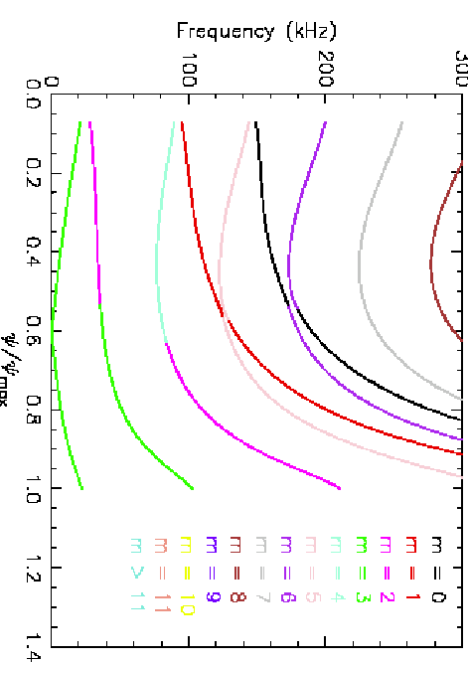
$n = 1$  mode family stellarator continua

dominant poloidal mode is color coded

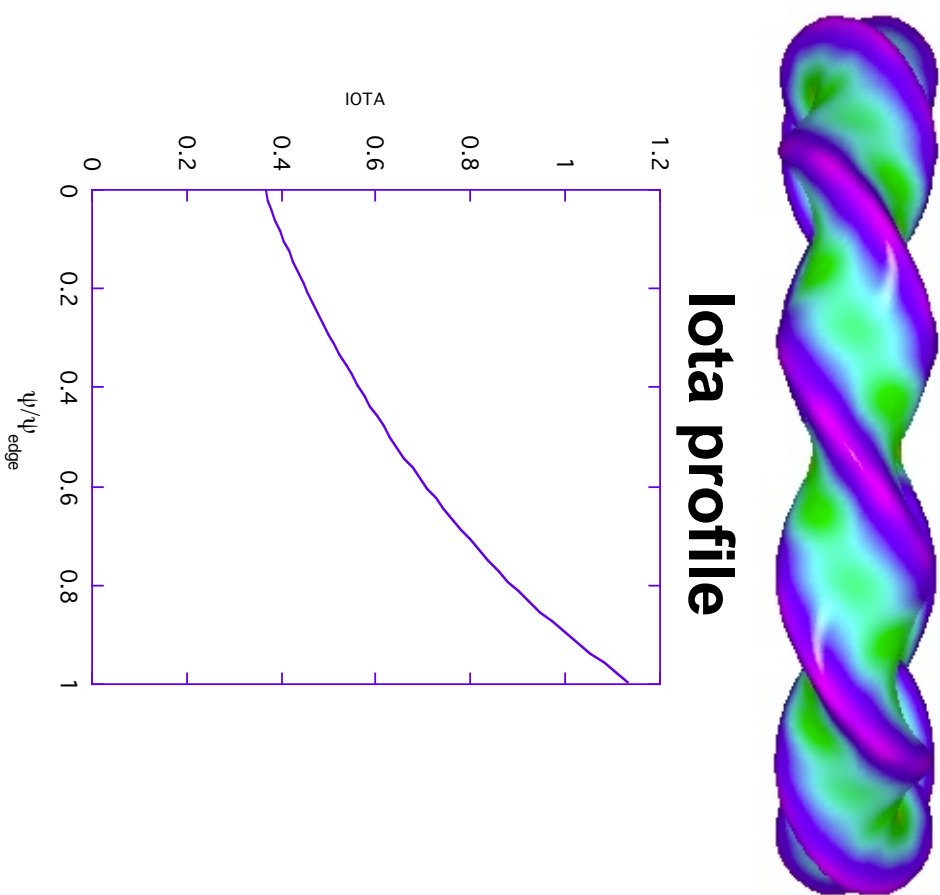


$n = 1$  mode family stellarator continua

dominant toroidal mode is color coded



# High aspect ratio torsatron LHD configuration



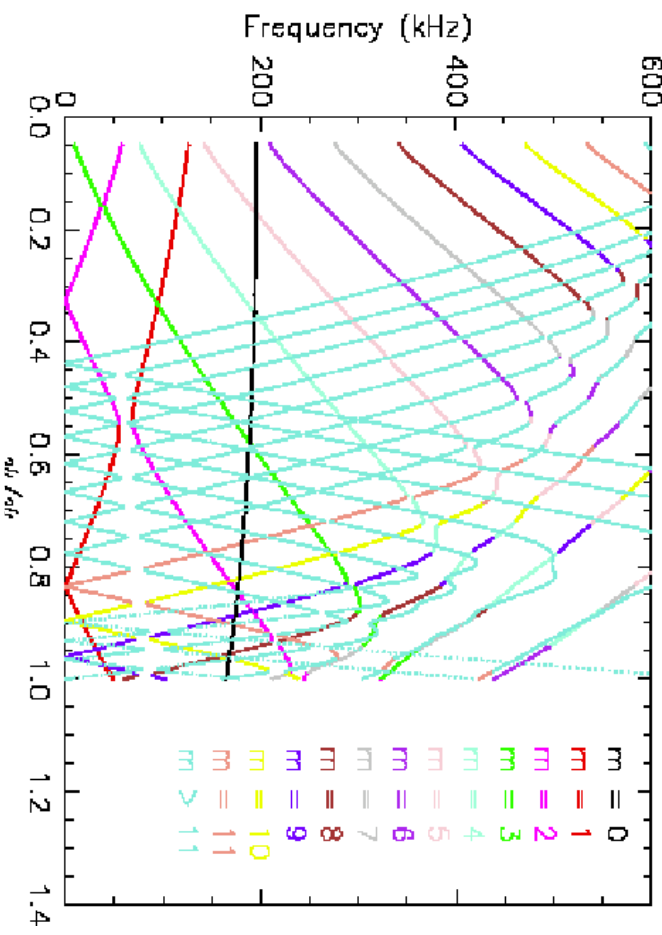
# LHD (10 field periods, $R/\langle a \rangle = 6$ , torsatron)

Continuum structure with 3D equilibrium coefficients, but only one ( $n = 1$ ) toroidal mode

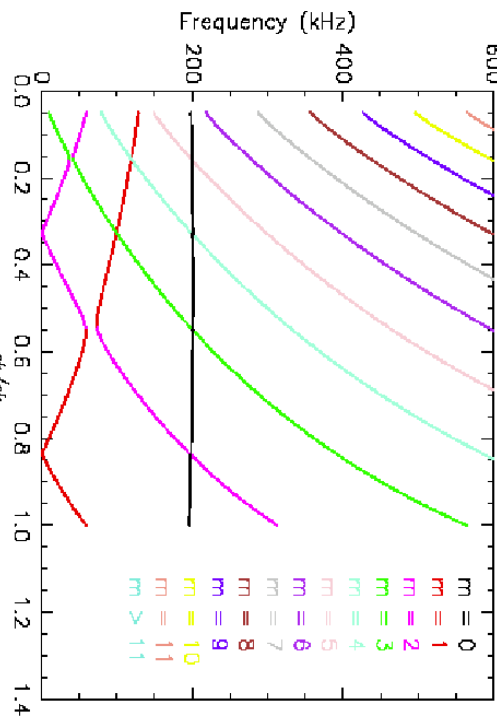
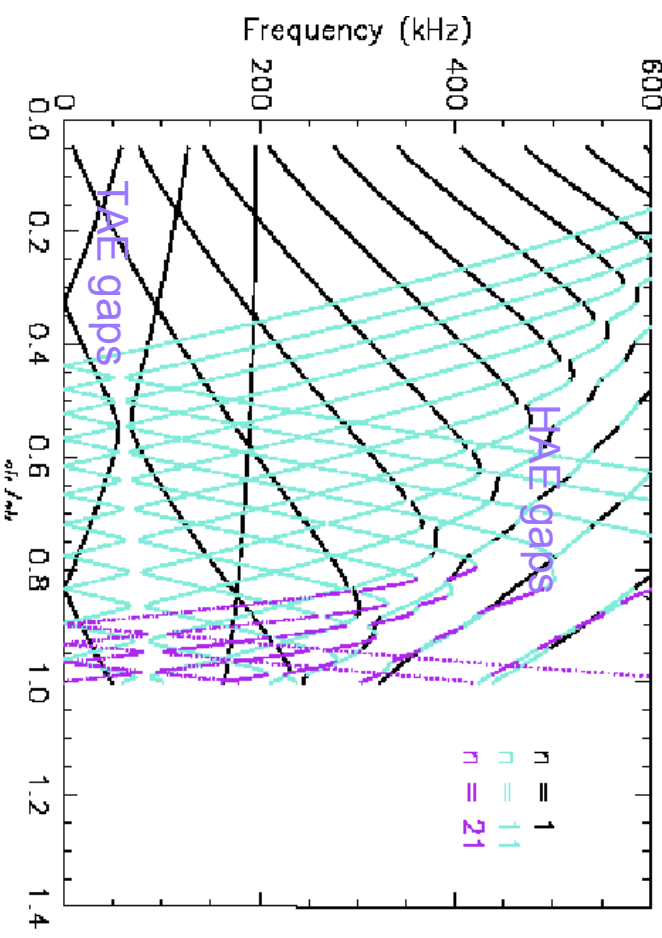
Continua with multiple toroidal modes



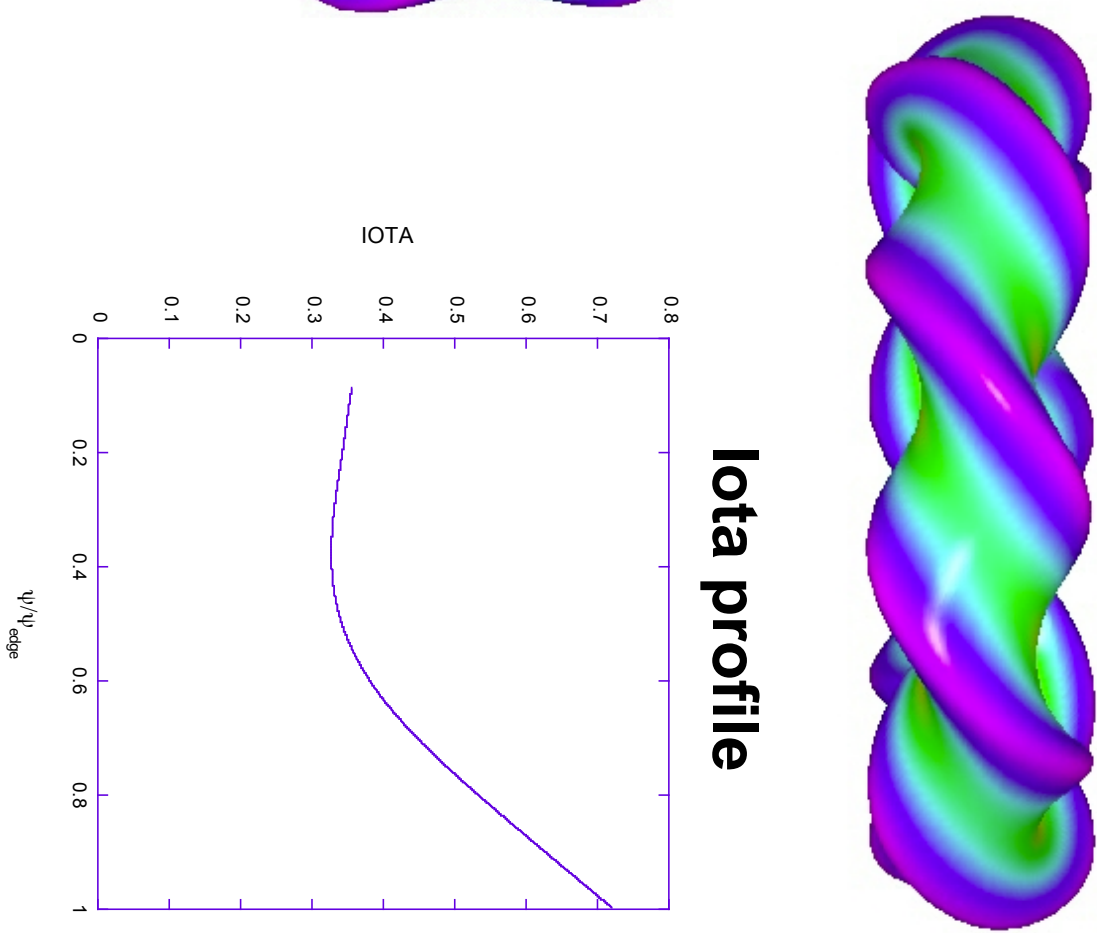
$n = 1$  mode family stellarator continua  
dominant poloidal mode is color coded



$n = 1$  mode family stellarator continua  
dominant toroidal mode is color coded



# CHS configuration

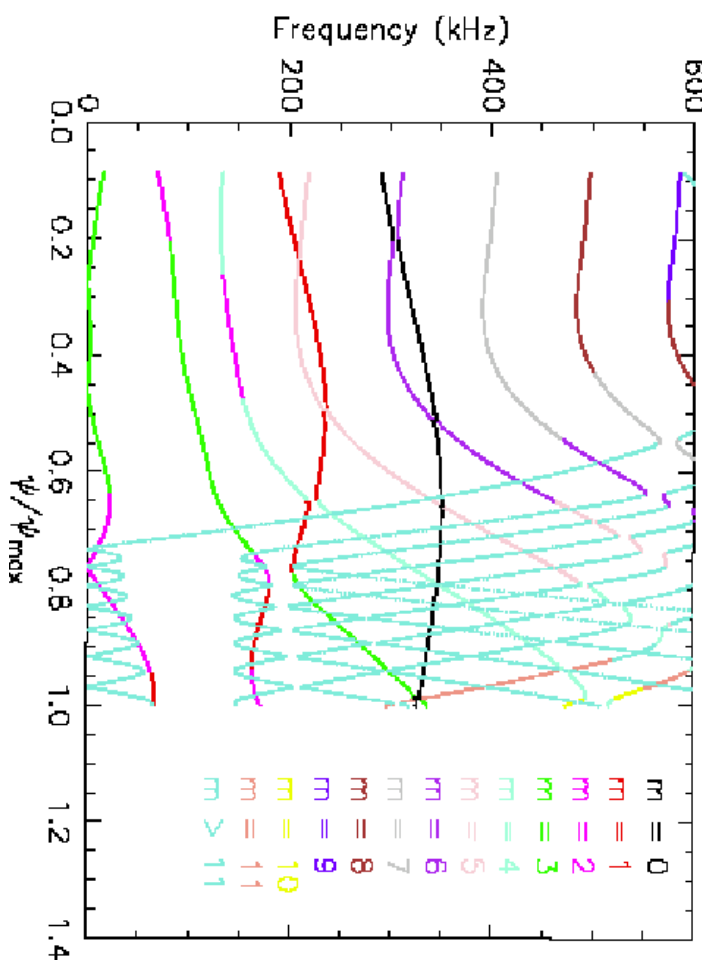


# CHS (8 field periods, $R/\langle a \rangle = 5$ , torsatron)

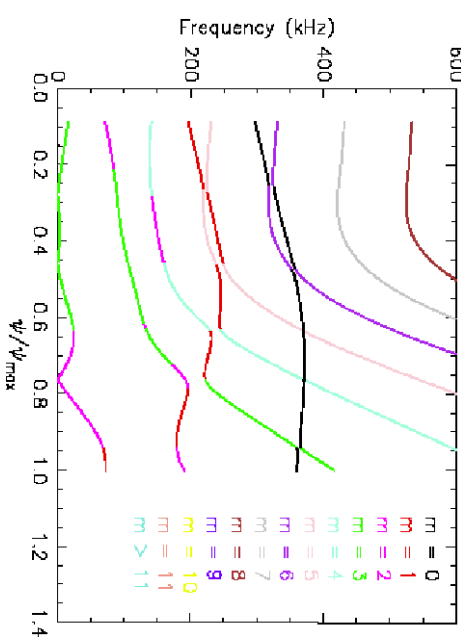
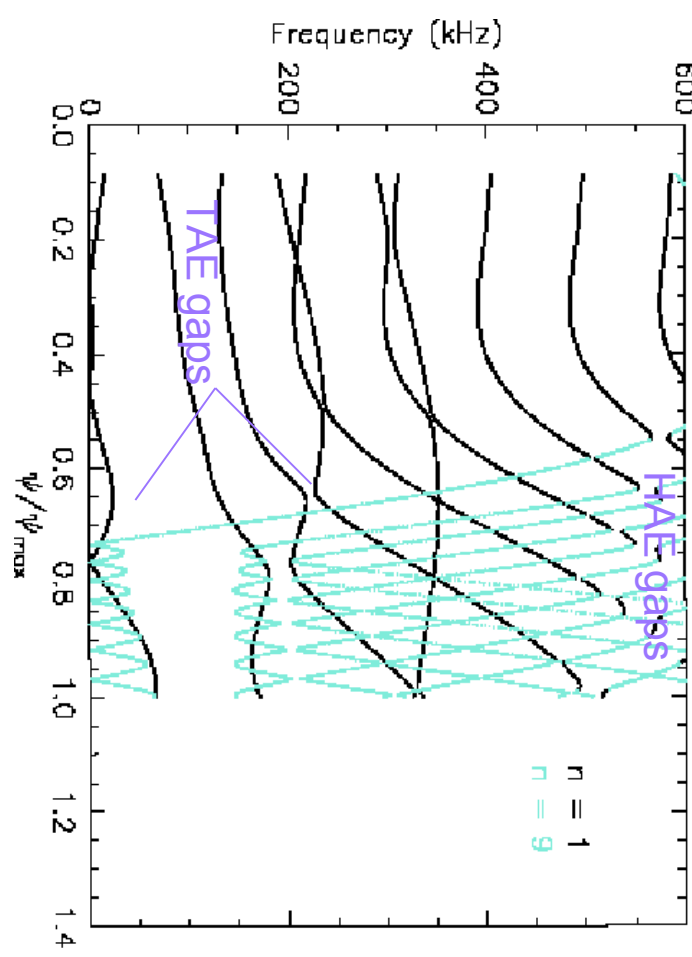
Continuum structure with 3D equilibrium coefficients, but only one ( $n = 1$ ) toroidal mode

Continua with multiple toroidal modes

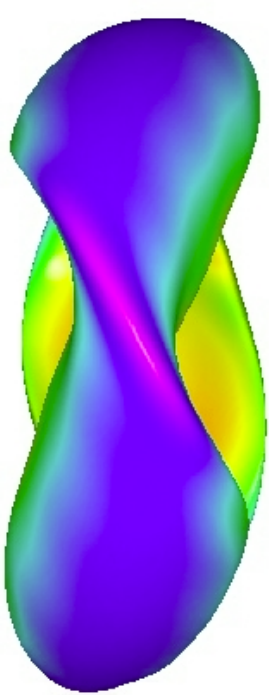
$n = 1$  mode family stellarator continua  
dominant poloidal mode is color coded



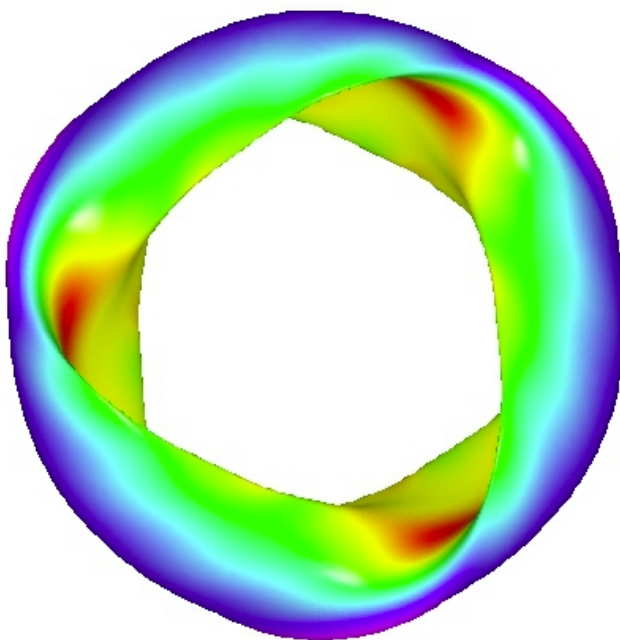
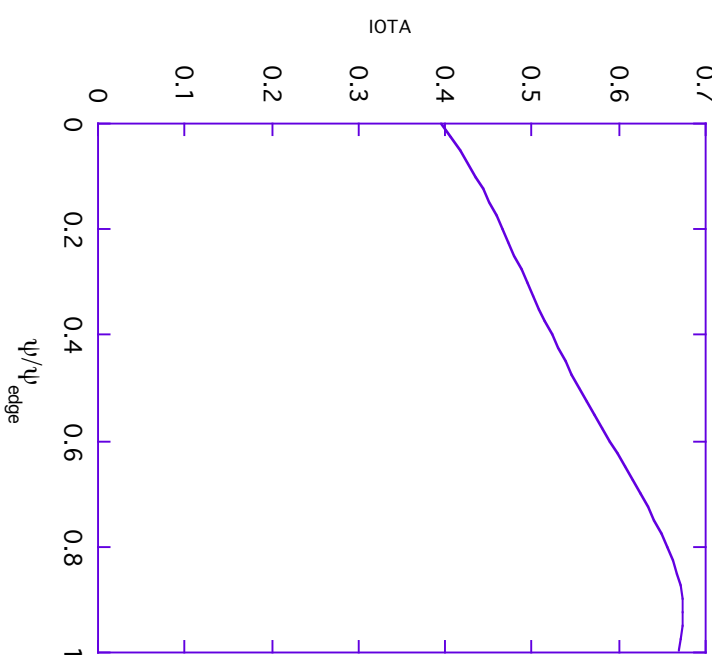
$n = 1$  mode family stellarator continua  
dominant toroidal mode is color coded



# Low aspect ratio quasi-toroidal configuration L|383



**Iota profile**



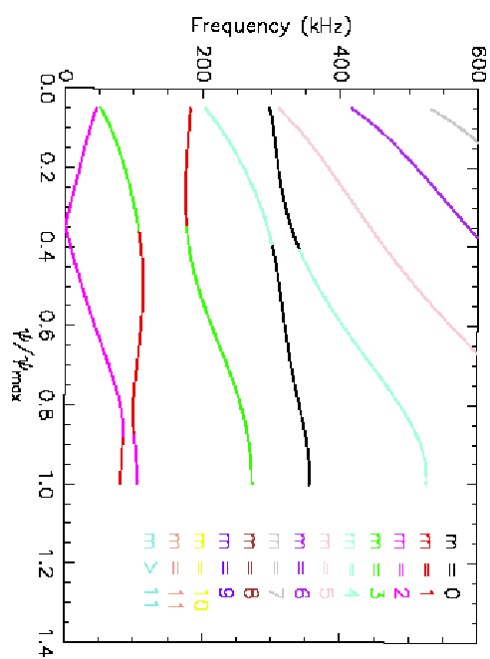
# NCSX (3 field period, $R/\langle a \rangle = 4.4$ , quas-toroidal symmetry)

Continuum structure with 3D equilibrium coefficients, but only one ( $n = 1$ ) toroidal mode

Continua with multiple toroidal modes

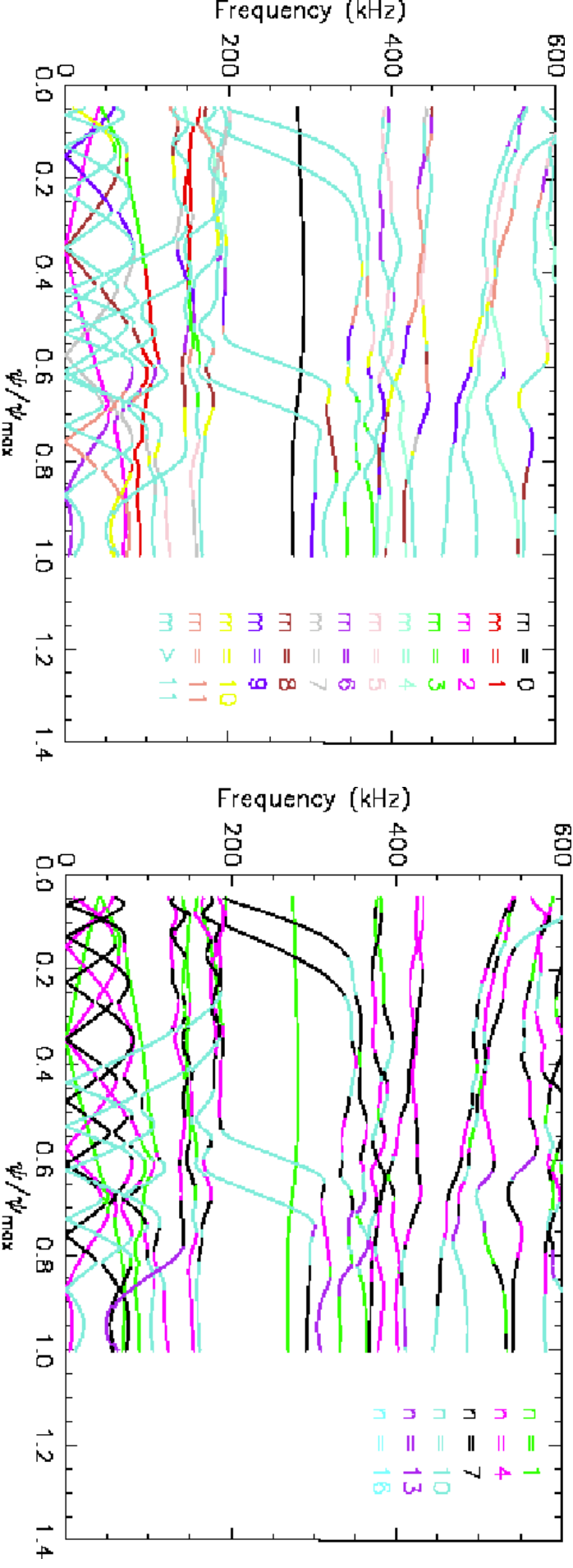
$n = 1$  mode family stellarator continua

dominant poloidal mode is color coded

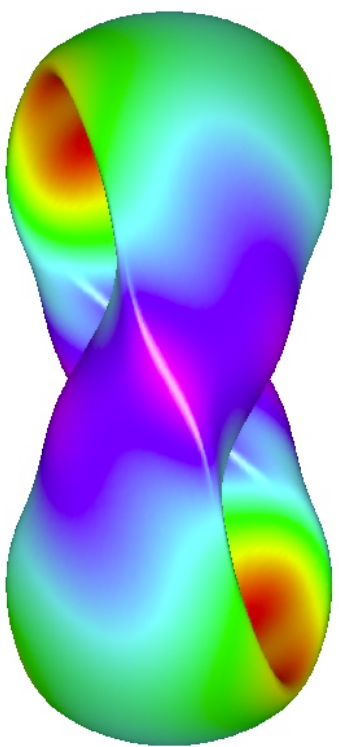


$n = 1$  mode family stellarator continua

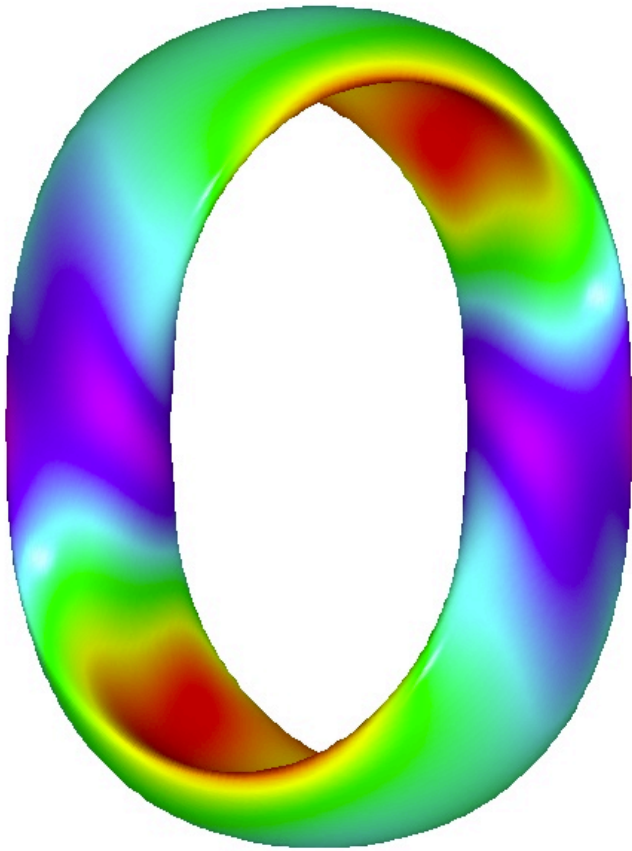
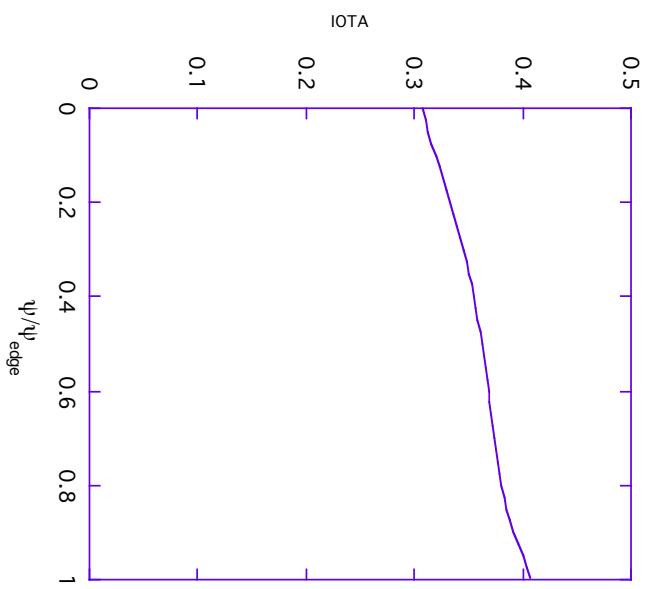
dominant toroidal mode is color coded



# Low aspect ratio quasi-poloidal configuration QPS



**Iota profile**



# QPS (2 field periods, $R/\langle a \rangle = 2.7$ , quasi-poloidal symmetry)

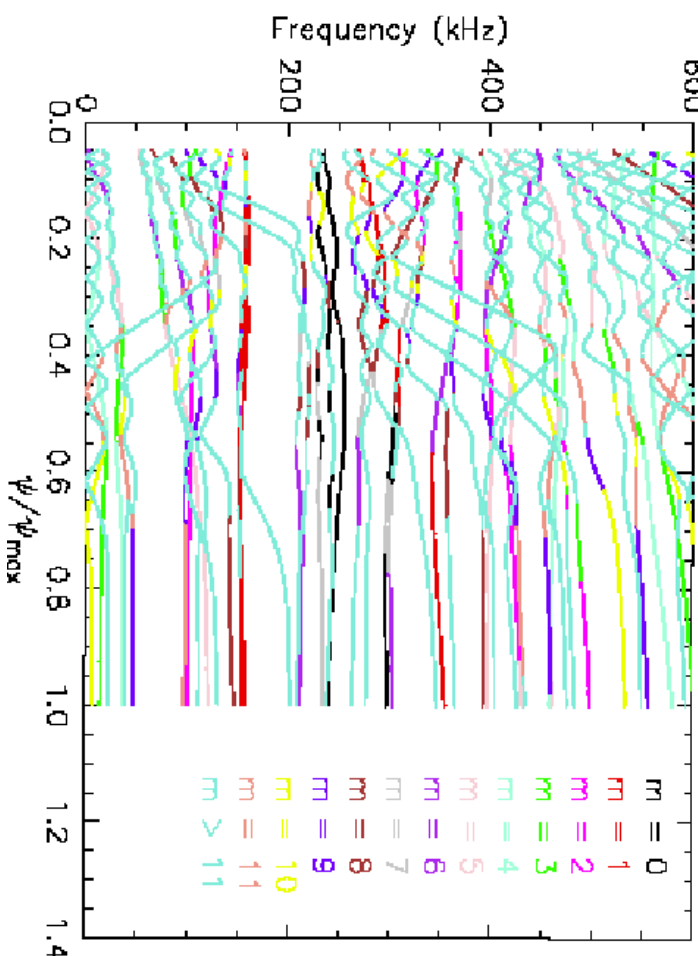
Continuum structure with 3D equilibrium coefficients, but only one ( $n = 1$ ) toroidal mode

Continua with multiple toroidal modes



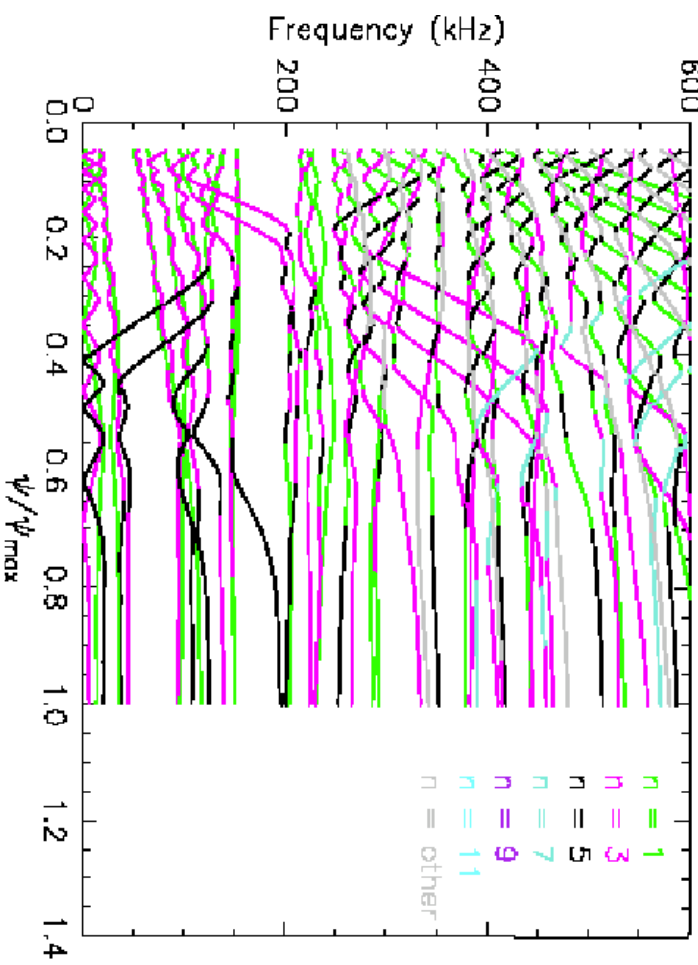
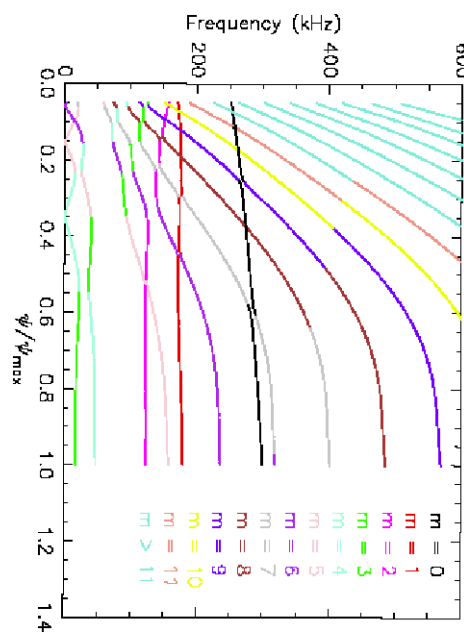
$n = 1$  mode family stellarator continua

dominant poloidal mode is color coded



$n = 1$  mode family stellarator continua

dominant toroidal mode is color coded



# Conclusions

- The 3-dimensional structure of stellarator equilibria introduce new mode couplings in the Alfvén continuum spectrum:
  - Helical Alfvén mode (HAE)  $n, m$  with  $n+N_{fp}, m + m_0$
  - Mirror Alfvén mode (MAE)  $n, m$  with  $n+N_{fp}, m$
- HAE modes are accessible at lower frequencies in compact systems (QPS, LI383)
  - Cross-linking of adjacent  $n$ 's may enhance continuum damping effects (i.e., less open gap structure)
- Efficient method for stellarator Alfvén continua
  - Straight field line coordinates and exact (analytic) convolutions preserve  $\vec{B} \bullet \vec{\nabla}(\ ) = 0$  on rational surfaces
  - Lower condition numbers than other methods that were tried
  - Solves for all eigenvalues

## Conclusions (contd.)

- 3-D effects only slightly change torsatron (LHD, CHS) continua away from that of the equivalent tokamak
- Open Alfvén gap structures persist in compact stellarators to higher frequencies ( $\sim \Box_{ci}$ ) than for similar tokamaks
  - potentially useful for direct channeling of energetic ion energy to core ions

## Next Steps

- Extend STELLGAP to solve the more complete system of equations for the discrete modes lying within the gaps.
- Develop methods for calculating linearized destabilization of these discrete modes by energetic particles.
  - compare mode structures and stability thresholds with stellarator experiments
  - apply to 3D effects on TAE's in tokamaks (ripple, internal tearing and kink modes)
- Optimization of stellarators for AE mode minimization
- Develop nonlinear models

# **Shear Alfvén Eigenmodes in Compact Stellarators**

D. A. Spong<sup>1</sup>, R. Sanchez<sup>2</sup>, S.P. Hirshman<sup>1</sup>, A. Weller<sup>3</sup>

<sup>1</sup>*Oak Ridge National Laboratory, P.O. Box 2009, Oak Ridge, TN 37831-8073*

<sup>2</sup>*Universidad Carlos III de Madrid, Madrid, Spain*

<sup>3</sup>*Max-Planck-Institut für Plasmaphysik, IPP-Euratom Association, Garching, Germany*

*43rd Annual Meeting of the APS Division of Plasma Physics*

*October 29 - November 2, 2001*  
*Long Beach, California*